

PAPER • OPEN ACCESS

Biohybrid generators based on living plants and artificial leaves: influence of leaf motion and real wind outdoor energy harvesting

To cite this article: Fabian Meder *et al* 2021 *Bioinspir. Biomim.* **16** 055009

View the [article online](#) for updates and enhancements.

You may also like

- [Bioinspired design and optimization for thin film wearable and building cooling systems](#)
Jonathan Grinham, Matthew J Hancock, Kitty Kumar et al.
- [An electret-based aeroelastic flutter energy harvester](#)
M Perez, S Boisseau, P Gasnier et al.
- [Two modes of motions for a single disk on the vibration stage](#)
Liyang Guan, Li Tian, Meiyong Hou et al.

Bioinspiration & Biomimetics

OPEN ACCESS



RECEIVED
19 March 2021

REVISED
3 July 2021

ACCEPTED FOR PUBLICATION
22 July 2021

PUBLISHED
13 August 2021

Original content from this work may be used under the terms of the [Creative Commons Attribution 4.0 licence](https://creativecommons.org/licenses/by/4.0/).

Any further distribution of this work must maintain attribution to the author(s) and the title of the work, journal citation and DOI.



PAPER

Biohybrid generators based on living plants and artificial leaves: influence of leaf motion and real wind outdoor energy harvesting

Fabian Meder^{1,*} , Serena Armiento¹, Giovanna Adele Naselli¹, Marc Thielen² , Thomas Speck^{2,3} and Barbara Mazzolai^{1,*}

¹ Bioinspired Soft Robotics, Istituto Italiano di Tecnologia, Viale Rinaldo Piaggio 34, Pontedera, Pisa 56025, Italy

² Plant Biomechanics Group, Botanic Garden, Faculty of Biology, University of Freiburg, Schänzlestraße 1, Freiburg 79104, Germany

³ Cluster of Excellence livMatS, Freiburg Center for Interactive Materials and Bioinspired Technologies (FIT), University of Freiburg, Georges-Köhler-Allee 105, Freiburg 78110, Germany

* Authors to whom any correspondence should be addressed.

E-mail: fabian.meder@iit.it and barbara.mazzolai@iit.it

Keywords: green energy, plants, triboelectric generators, leaf fluttering, autonomous energy sources, wind power

Supplementary material for this article is available [online](#)

Abstract

Plants translate wind energy into leaf fluttering and branch motion by reversible tissue deformation. Simultaneously, the outermost structure of the plant, i.e. the dielectric cuticula, and the inner ion-conductive tissue can be used to convert mechanical vibration energy, such as that produced during fluttering in the wind, into electricity by surface contact electrification and electrostatic induction. Constraining a tailored artificial leaf to a plant leaf can enhance oscillations and transient mechanical contacts and thereby increase the electricity outcome. We have studied the effects of wind-induced mechanical interactions between the leaf of a plant (*Rhododendron*) and a flexible silicone elastomer-based artificial leaf fixed at the petiole on power output and whether performance can be further tuned by altering the vibrational behavior of the artificial leaf. The latter is achieved by modifying a concentrated mass at the tip of the artificial leaf and observing plant-generated current and voltage signals under air flow. In this configuration, the plant-hybrid wind-energy converters can directly power light-emitting diodes and a temperature sensor. Detailed output analysis has revealed that, under all conditions, an increase in wind speed leads to nearly linearly increased voltages and currents. Accordingly, the cumulative sum energy reaches its highest values at the highest wind speed and resulting oscillations of the plant-artificial leaf system. The mass at the tip can, in most cases, be used to increase the voltage amplitude and frequency. Nevertheless, this behavior was found to depend on the individual configuration of the system, such as the leaf morphology. Analysis of these factors under controlled conditions is crucial for optimizing systems meant to operate in unstructured outdoor scenarios. We have established, in a first approach, that the artificial leaf-plant hybrid generator is capable of autonomously generating electricity outdoors under real outdoor wind conditions, even at a low average wind speed of only 1.9 m s^{-1} .

Introduction

Living plants acting as autonomous energy sources might produce sufficient power to drive low-power electronics and are thus a ‘green’ technology vision for the replacement of batteries and for emission-free resource-saving energy harvesting [1]. Interestingly, the materials and the structural arrangements in leaves and living plant tissue have recently been

shown to provide an assembly that can be used to convert mechanical energy produced by wind and rain into electricity [2–6]. The ongoing advancement of the understanding, adaptation and manufacture of materials allows new combinations between artificial components and living organisms enabling exciting strategies that have the potential for creating multiple synergies between plants and man-made technologies. Indeed, a new generation of plant-hybrid

systems is benefitting from specific material/tissue properties and functionalities of living plants with applications ranging from energy harvesting to sensing [7–14].

The goal of producing electricity in combination with living plants has been achieved by implementations such as plant microbial fuel cells [15–21] and glucose biofuel cells [22, 23]. In these examples, organic molecules provided by the plant are indirectly (with the help of bacteria in the soil) or directly (using plant sap glucose) converted into electricity by an artificial fuel cell. Thus, energy conversion is carried out by an artificial device. In addition, plants have recently been reported to be able directly to convert mechanical energy and wind energy into electricity using a tissue-intrinsic structure without the need for an extrinsic energy converter [2, 3]. This energy conversion is solely based on the materials of the plant and their structural arrangement. However, whether a physiological active mechanism is involved in this effect remains unclear. In detail, plant leaves are covered with a thin polymer layer that is several micrometres thick and is called the cuticle [24]. Because of its chemical structure (consisting of multiple waxes and lipids) [24, 25], it acts as a dielectric material and can accumulate charges upon contact with another material through contact electrification [2]. Following well-known principles of contact electrification [26], certain material pairs produce higher charging than when materials of similar chemical structure come into contact. Indeed, materials such as polytetrafluoroethylene and silicone rubber have been previously shown to lead to significant charging in combination with plant cuticle [2, 4]. Moreover, the plant provides a water- and ion-containing cellular tissue underneath the cuticle. The charges created on the cuticle are electrostatically induced into the ion-conductive tissue leading to a current that can be harvested by insertion of an electrode into the plant tissue. In this configuration, living plants constitute single electrode triboelectric generators (TEGs). During the past few years, TEGs made of artificial materials have been demonstrated to be a possible energy source for the Internet of Things and wearable sensors. They have also been considered for use in larger scale energy harvesting farms with reported power densities of up to several 100 watts per square meter of active surface area [27–29]. If living plants can also be used as such generators, then artificial material consumption could be reduced. Nevertheless, the intrinsic properties of plants, which include O₂ generation, CO₂ fixation, dynamic self-repair and provision of a biosphere for animals and insects, occur naturally and are extremely difficult to realize (if at all) in artificial generators. Figure 1(a) shows a typical configuration of the plant-hybrid generators. An artificial leaf is assembled on the plant; it consists of a suitable dielec-

tric material that (1) creates high charging, (2) lies in contact with the plant tissue and (3) is applied to an electrode that is ideally translucent in order for the plant unobstructedly to perform photosynthesis. The mechanism of energy conversion is schematized in figure 1(b), which shows essential components and charge distributions. The energy harvesting capability exists in this manner theoretically in all land plants bearing a polymeric cuticle with adjacent conductive cellular tissue and the effect has been confirmed in at least eight different plant species with different efficiencies [2]. Some of the best performing species in this study are species such as *Rhododendron* sp. and *Nerium oleander* because of their mechanically robust leaves that sustain the mechanical impacts required for charge generation. Power outputs achieved to date by plants have been high enough for single leaves to drive multiple (more than 100) light emitting diodes (LEDs) and sensors [2–5]. This offers an exciting opportunity for converting plants into devices capable of energy harvesting when certain issues can be solved. The artificial components of the plant-hybrid systems now have to be tailored, adapted and optimized in order to achieve the best power outputs by optimally exploiting environmental wind energy. One article has reported the application in wind-energy harvesting and the use of plants in combination with artificial leaves that move by wind [3]. Wind speed and wind direction have been shown to affect such a system clearly establishing that a cross-flow arrangement of the leaf and the wind direction leads to the highest outputs that increase with wind speed. Nevertheless, whether an artificial leaf can itself be optimized to interact with a highly unstructured plant and its inherent natural variability in order to tailor the related mechanics that will lead to the energy conversion remains unknown. Moreover, such systems have never been tested outdoors under real wind conditions.

We have modified plants with transparent artificial leaves made of silicone rubber and an indium tin oxide (ITO) electrode on polyethylene terephthalate (PET), see figures 1(c) and (d). Furthermore, we have varied a concentrated mass applied at the tip of the artificial leaf structure in order to observe the way that the complex aerodynamic oscillatory behaviour manifested in plant-produced current and voltage signals is influenced under a range of wind speeds. Our investigation has led to important conclusions with regard to those parameters that affect the interaction between the artificial leaves and the plant leaves under airflow and wind excitation and suggests design directions for possible plant-hybrid energy converters. We also show, for the first time, that the system can harvest energy by converting real outdoor wind. Furthermore, we confirm that plant-hybrid generators are capable of directly powering 150 LEDs and a digital thermometer from wind energy.

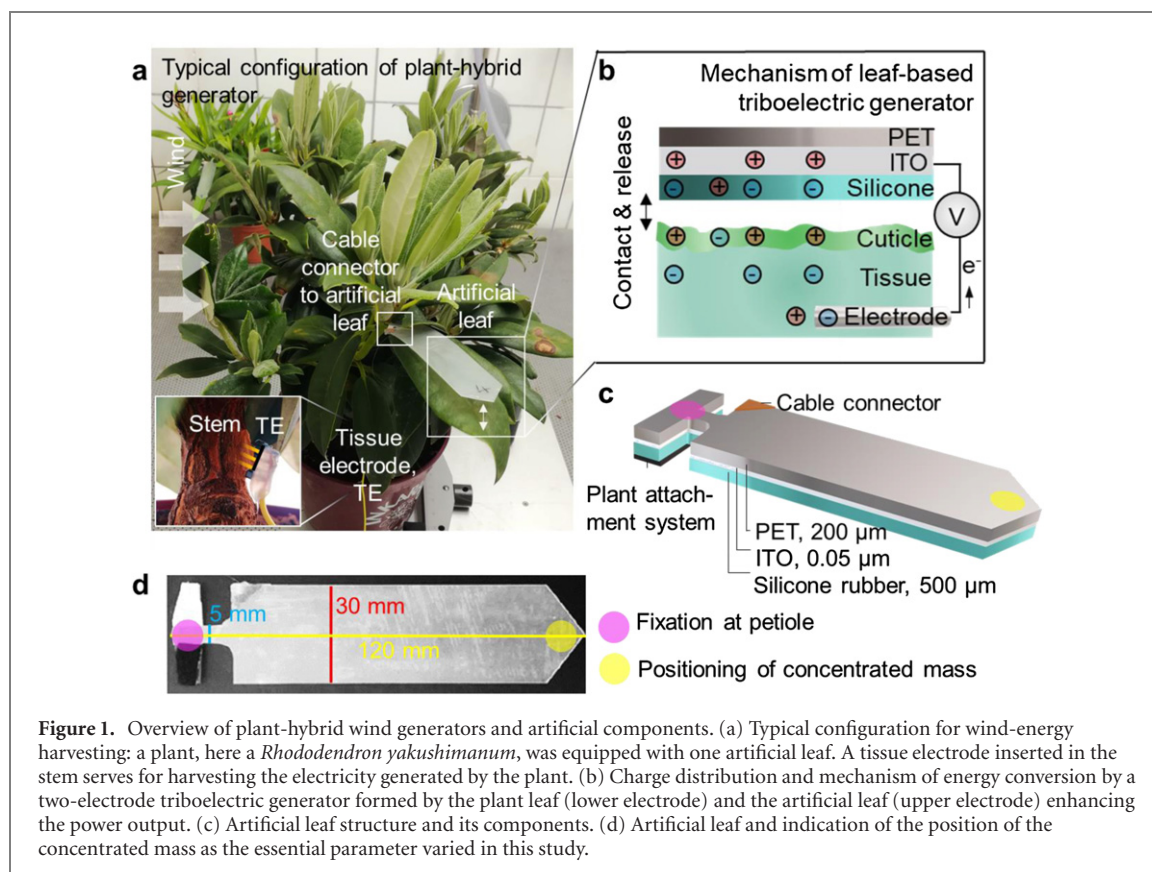


Figure 1. Overview of plant-hybrid wind generators and artificial components. (a) Typical configuration for wind-energy harvesting: a plant, here a *Rhododendron yakushimanum*, was equipped with one artificial leaf. A tissue electrode inserted in the stem serves for harvesting the electricity generated by the plant. (b) Charge distribution and mechanism of energy conversion by a two-electrode triboelectric generator formed by the plant leaf (lower electrode) and the artificial leaf (upper electrode) enhancing the power output. (c) Artificial leaf structure and its components. (d) Artificial leaf and indication of the position of the concentrated mass as the essential parameter varied in this study.

1. Materials and methods

1.1. Plant species

Rhododendron yakushimanum was provided by the Botanic Garden, University of Freiburg, Germany. *Rhododendron* hybrid ‘Marcel Menard’ was purchased from a plant nursery. The plants were either kept outdoors and watered once per week or kept in a phyt chamber with lighting under a 16 h day and 8 h night cycle.

1.2. Fabrication of artificial leaves

Artificial leaves as displayed in figures 1(c) and (d) were made as follows. Transparent ITO-coated PET films (thickness 200 μm , nominal sheet resistance 350–500 Ω per square, Thorlabs Inc., USA) were coated with a thin layer of silicone rubber adhesive (Sil-PoxyTM, Smooth-On Inc., USA) applied onto the ITO layer by means of a doctor blade. Immediately thereafter, a layer of translucent silicone rubber was positioned on top of the glue layer (thickness 500 μm , obtained from Modulor GmbH, Germany, previously washed with isopropyl alcohol and wiped dry by using dust-free tissue) followed by drying for a minimum of 24 h. The multilayer sheets were cut into the desired shapes by using a laser cutter (VersaLaser VLS3.60, Universal Laser Systems Inc., USA). To affix the artificial leaves to the petioles of the leaves of a plant, either a self-adhesive Velcro[®]-based attachment system was glued onto the artificial leaf or the artificial leaf was taped with silicone adhesive tape to the

petiole. In addition, in order to connect the ITO electrode, the silicone film was carefully lifted from the ITO electrode at one corner, and a piece of copper tape with conductive glue was attached to the ITO layer. Subsequently, a cable was soldered to the copper tape, and the silicone layer was returned to its original position and re-affixed using the silicone adhesive. All cutting edges were sealed with silicone. The leaves were fixed at the petioles of the natural leaves to obtain biohybrid plant energy harvesters as shown in figure 1(a).

1.3. Indoor experiments at various wind speed

Initially, experiments were performed in a specialized phyt chamber (height: 2.13 m, depth: 2.75 m, width: 2.5 m) equipped with an active climate control system and a wind source consisting of 96 individually adjustable nozzles that allowed the wind speed and direction, the temperature, and the humidity to be controlled during the experiments. Plants were exposed to a controlled air flow at a temperature of 22 ± 1 $^{\circ}\text{C}$, a relative humidity (RH) of $50 \pm 3\%$, and continuous lighting during the experiments and to 8 h dark phases in which no experiments were conducted. A ventilation system (MUB 042-500DV-A2, Systemair, Skinnskatteberg, Sweden (max speed: 1330 rpm)) in combination with a frequency converter (VLT[®] HVAC Drive FC 102, Danfoss, Nordborg, Denmark) was employed to control the wind speed. The nozzles releasing the controlled air flow were all oriented towards the plant, which was placed

in a distance of ~ 50 cm from the nozzles (measured from the plant center). In further experiments, the plants were each placed in a Faraday cage, and wind was blown onto the plant from a tube (diameter: 8 mm) connected to a compressed air source. The plant was placed at a distance of ~ 1 m from the tube outlet at a fixed position. Flow speed was controlled with a pneumatic regulator. Each time that the wind speed was set, the actual wind speed at the individual leaves under analysis was simultaneously measured at a distance of ~ 3 cm in front of the leaf by using a hot wire anemometer (405i, Testo SE & Co. KGaA, Germany). Experiments were performed at an average temperature of ~ 25 °C and RH of $\sim 50\%$. Procedures for electrical signal acquisition are described below.

1.4. Measurements and data acquisition

All measurements were performed on healthy potted plants. A gold-coated pin electrode was inserted into the stem of the plant (see figure 1) to measure and harvest signals generated by the plants. Voltages were measured with an oscilloscope (MSO7014A, Agilent Technologies, USA) equipped with a passive 10 M Ω probe. Short circuit currents were measured using a high input impedance electrometer (6517B, Keithley, USA). Data from up to eight artificial leaves installed on the same plant were recorded using the plant tissue electrode and the ITO electrode of the artificial leaf by using the circuit indicated in figure 1(b). Each leaf was tested in at least three to five replicates over a period of typically 25 s of data acquisition at high resolution (10^6 samples/measurement) by recording up to approximately 200 current/voltage peaks per leaf (the mean and standard deviation of the amplitude are reported). All data were analyzed and plotted using Matlab, Version R2019b. Leaf movements were video-recorded at 240 fps with a GoPro Hero7 camera, and oscillations were analyzed by either automatic tracking (using colored markers applied at the tip of the artificial and natural leaves) or manual tracking of the plant and artificial leaf tips by using the software Tracker, Version 5.1.3. Local derivatives of the vibrational profiles were obtained using Matlab, Version R2019b to extract approach and contact events of the artificial and natural leaves ('bar codes') and to plot the data. To harvest and record energy simultaneously from eight leaves outdoors, a customized data acquisition circuit was used in which eight individual ceramic capacitors (1 μ F, 16 V, Taiyo Yuden Co. LTD., Japan) were charged by the generated signals after diode bridge rectification. The circuit automatically measured the voltage across the capacitors and discharged the capacitors when a certain set threshold voltage (typically 2 V in our experiments) was reached. The voltage across the capacitors was tracked at a frequency of 1 Hz for about 1 h.

2. Results

2.1. Correlation of leaf oscillations and plant-generated voltages

The relative motion between the artificial and the natural leaves leads to the contact events required for the contact charging of the cuticle and the artificial leaf and thus to energy harvesting. To confirm this correlation, we exposed a *R. yakushmanum* plant modified with a single artificial leaf as shown in figure 1 to various air flows (1.4, 3.1, and 4.8 m s $^{-1}$ average wind speed). The air was blown, in this case, in a cross-flow orientation in relation to the artificial leaf-leaf couple from 96 nozzles (~ 30 mm diameter) towards the plant in a phytochamber with controlled relative humidity (RH = $50 \pm 3\%$) and temperature ($T = 22 \pm 1$ °C) and continuous lighting. Figure 2(a) shows the voltage signals, V_m , generated by the plant and the artificial leaf in air flow when measured at a pin electrode inserted in the plant tissue. In addition, the related cumulative sum of the energy $E = \frac{V_m^2 t}{R_i}$ over the measurement period is shown, with t being the data acquisition period and R_i being the inner resistance of the plant-hybrid generator assuming a value of 70 M Ω as determined earlier for a similar system [3]. The graphs show that higher wind speeds lead to an increase in the obtained V_m amplitude, and correspondingly that E increases. In the 'bar codes' under the voltage plots, a single bar corresponds to a positive maximum in V_m resulting from the separation of the artificial leaf and the leaf surface after prior contact. The number of bars indicates the frequency of the maxima that is increasing with the wind speed at a rate of ~ 0.74 per 1 m s $^{-1}$. Indeed, alteration of the wind speed from 1.4 to 3.1 m s $^{-1}$ leads to an increase of the frequency by 1.24, and an change from 3.1 to 4.8 m s $^{-1}$ leads to a frequency increase of 1.27.

Moreover, the motions of the natural and the artificial leaf were tracked at their tips, by using video analysis of high-speed video recordings of the hybrid plant under wind excitation, from leaf motions such as those shown in video S1 (<https://stacks.iop.org/BB/16/055009/mmedia>). Figure 2(b) shows the absolute motions of the natural (green) and the artificial leaf (blue). The oscillations of the artificial and the *R. yakushmanum* leaf describe generally similar curves in terms of amplitudes, frequency, and time period, and the amplitudes increase with increasing wind speed. This behavior can be expected from the voltage signals obtained, which also increase with wind speed. A further analysis is provided by the bar codes in the graphs. The bars indicate the events in the vibrational profiles when the plant leaf performs an upward motion, and the artificial leaf moves simultaneously downwards, determined by analyzing the local derivatives of the vibrational profiles. Such events lead expectably to a transient contact between the two leaves

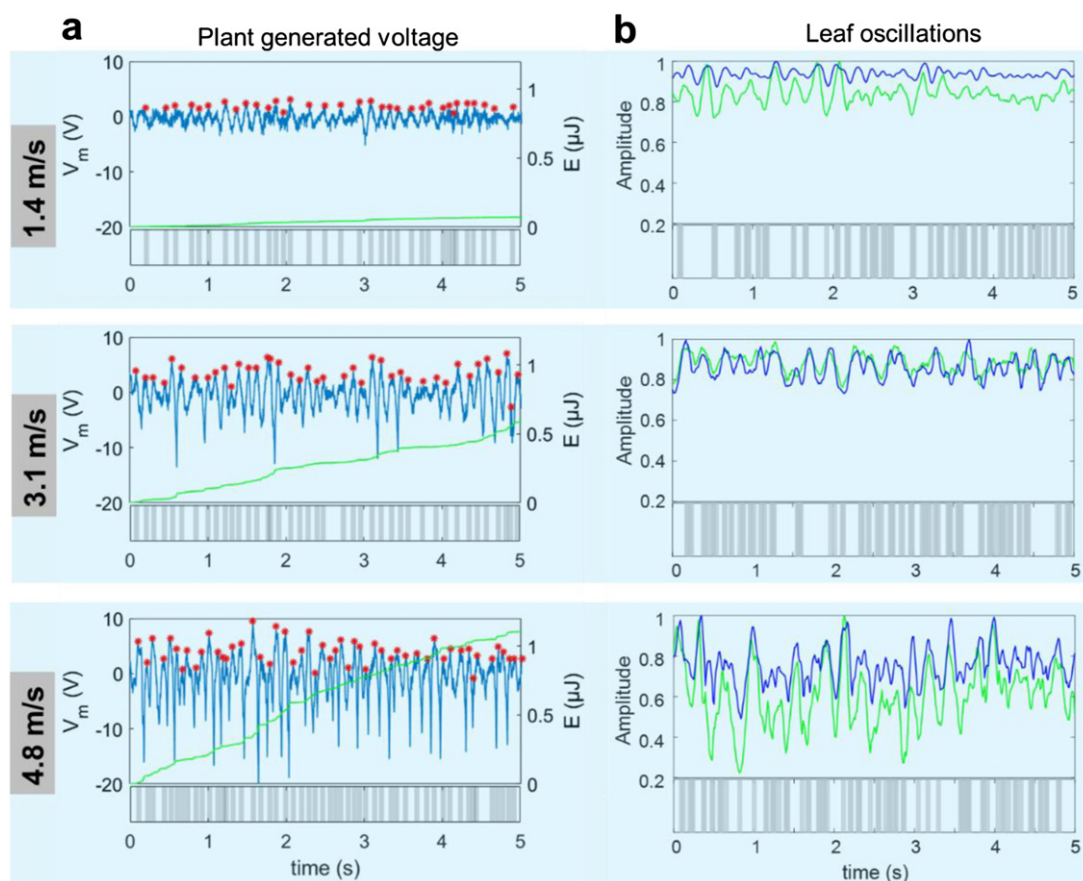


Figure 2. Correlation of plant-generated voltage and the leaf oscillations. (a) The three graphs represent the alternating voltage peaks V_m generated in *R. yakushmanum* equipped with a single artificial leaf during exposure to a controlled wind source as a function of wind speed (1.4, 3.1, and 4.8 m s^{-1}). Positive peaks that occurred when the plant leaf and the artificial leaf separated after prior wind-induced contact were tracked to obtain an indication of the frequency of contact events (red stars and the gray bars highlight the positive V_m peaks). The green line shows the related cumulative sum energy as a function of time. (b) Tracking the normalized amplitude (in mm) of the leaf motions showing the oscillations of the plant leaf (green) and the artificial leaf (blue) at the given wind speeds. The gray bars in the lower panel indicate the frequency of contact events between the artificial and the natural leaf. The events in the vibrational profiles when the plant leaf travels upwards and the artificial leaf moves simultaneously downwards leading to a transient contact were tracked by analysis of the local derivatives of the curves.

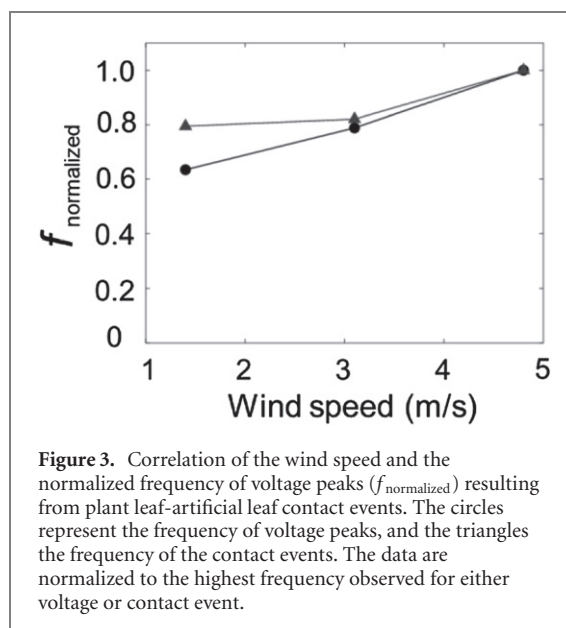
and is followed by separation; this is required for effective contact electrification and electrostatic induction.

Figure 3 illustrates the correlation between the frequency of V_m peaks representing the plant-generated electricity and the frequency of the oscillations that lead to contact charging. The graph confirms that vibrational amplitudes and contact-separation frequencies increase with wind speed and correspondingly create higher voltage signals. A general simplified description of this leaf-artificial leaf configuration would hence be two oscillators that are constrained at one point at the petiole. Optimizing the artificial component such as by tailoring its natural frequency might thus be an option further to elevate the power generation. However, this requires additional essential understanding of highly complex dynamics. Plant behavior and factors such as branch movements, wind-induced rotation of leaves and streamlining, turbulent air flows influenced by other leaves and branches, frequency-dependent viscoelastic properties, and internal

damping will further influence the mechanical system. We therefore analyzed the way that the mechanical behavior of the artificial leaf affects signal generation in terms of voltage, current, and frequency of generated peaks.

2.2. Effect of concentrated mass at tip of artificial leaf on plant-generated signals

Figure 4(a) illustrates the leaf-artificial leaf combination. It depicts the factors that likely play a role in creating the overall mechanical behavior and the forces affecting contact electrification $\sum F$ (here expressed as a multivariable function to summarize the multifactorial dependency of the unstructured interaction between the artificial and the plant leaf). $\sum F$ is expected to result from the behavior of the plant stem (or whole plant) to which the leaf is attached, the petiole fixation point (as a point of constraint between the artificial leaf and the plant leaf), the artificial leaf (structure, shape, mechanics), the added weight at the tip of the leaf (parameter varied in this study), the plant leaf (its individual shape,



structure, size, mechanics), and the wind (speed, direction). These parameters are themselves clearly determined by multiple intrinsic factors, such as the individual shape of the plant leaf or the actual air flow and turbulences that a single leaf experiences and that are determined by other leaves in its surrounding or the wind direction as previously shown [3]. To investigate in more depth those parameters playing key roles, we equipped a *Rhododendron* plant with an artificial leaf and exposed it to various wind speeds as described above. Now, however, the same leaf was modified by having a concentrated mass at its tip indicated as 0 g (no additional weight), 0.5 g, 1 g, 1.5 g, or 2 g and was tested at three different wind speeds (1.4, 3.1, and 4.8 m s⁻¹). The concentrated mass at the tip of the flexible artificial leaf was expected to affect oscillation behavior in terms of reducing frequency but possibly to provoke higher impact forces attributable to larger contribution of inertia.

Figure 4(b) is a curve matrix representing the voltage peaks as a function of wind speed and added mass highlighting the positive and negative peaks (black and red circles, respectively) and their averages (green lines). The cumulative sum energy in the acquisition period is also given. The current signals measured under the same conditions are provided in supporting figure S1. The results indicate that the wind speed and the mass influence the electricity generated by the plant-hybrid system as expected. Figures 4(c) and (d) summarize the obtained voltage and current amplitude, respectively, as a function of wind speed, confirming that, under all conditions, an increase in the wind speed leads to almost linearly increased voltages and currents. Accordingly, the cumulative sum energy also reaches its highest values at the highest wind speed. For the leaf under investigation, the highest signals were observed with the highest concentrated mass added. Another important factor was the

frequency of voltage and current signals generated as given in figures 4(e) and (f), respectively. Current and voltage measurements were not directly correlated as they had been obtained in independent experiments performed directly after each other with the same leaf and wind conditions. The results show that the frequency increases with wind speed in cases of no added mass. However, under the given conditions, namely the addition of a mass (in particular, 2 g) at the tip of the artificial leaf, higher frequencies were observed, even at lower wind speeds. This is attributable to smaller amplitudes of movement (see video S2) that do not accompany higher voltages and currents, a phenomenon likely related to the lower impact forces obtained at these wind speeds, because leaf charging is impact-force-dependent [2].

The behavior is, as expected, strongly dependent on the plant leaf onto which the artificial leaf is fixed. Figure 5(a) compares the voltages and frequencies obtained from four different configurations in which the same artificial leaves with different added masses were attached to four different *Rhododendron* leaves on one and the same plant and exposed to alternating wind speeds coming from a fixed (cross flow) direction. Again, higher wind speeds led, for all leaves, to higher V_m , further confirming wind speed as being a key parameter for the system. The added mass also had an influence on the voltage amplitude. However, whether it led to a voltage increase or decrease depended in a rather complex manner on the leaf configuration/combination. In three of four cases, the added weight at the leaf tip increased the voltage amplitude.

Figure 5(b) presents the frequencies at which the voltage peaks occur for the four leaves investigated. A general trend that can be observed for three out of four leaves (leaf 1–3) is that frequency increases with wind speed, but that the greatest added mass (2 g) does not give the highest frequencies. Instead, the results suggest that the added mass of 1 g in all three cases led to a frequency close to the maximum and, at least for leaf 1 and 2, also to the highest voltage amplitudes. The frequency of voltage signals was different for leaf 4. Interestingly, the frequency decreased at higher wind speeds and was almost constant for all added masses. This behavior was likely caused by the shape of the *Rhododendron* leaf with its downward bending margins and its midrib lying at the highest point of the leaf blade (see also video 3). Thus, the midrib is closest to the artificial leaf, whereas the leaf blades on the left and the right are downward bending and more distant (figure 5(c)). Interestingly, stronger wind separated the artificial leaf and the plant leaf in a manner such that contact between the two surfaces was hampered. Added mass was not sufficient to balance this effect. The relevant motions of the leaves can be seen in video S3, which also shows the movements of leaf 1 with its lower intrinsic bending leading to high frequency contacts at higher wind

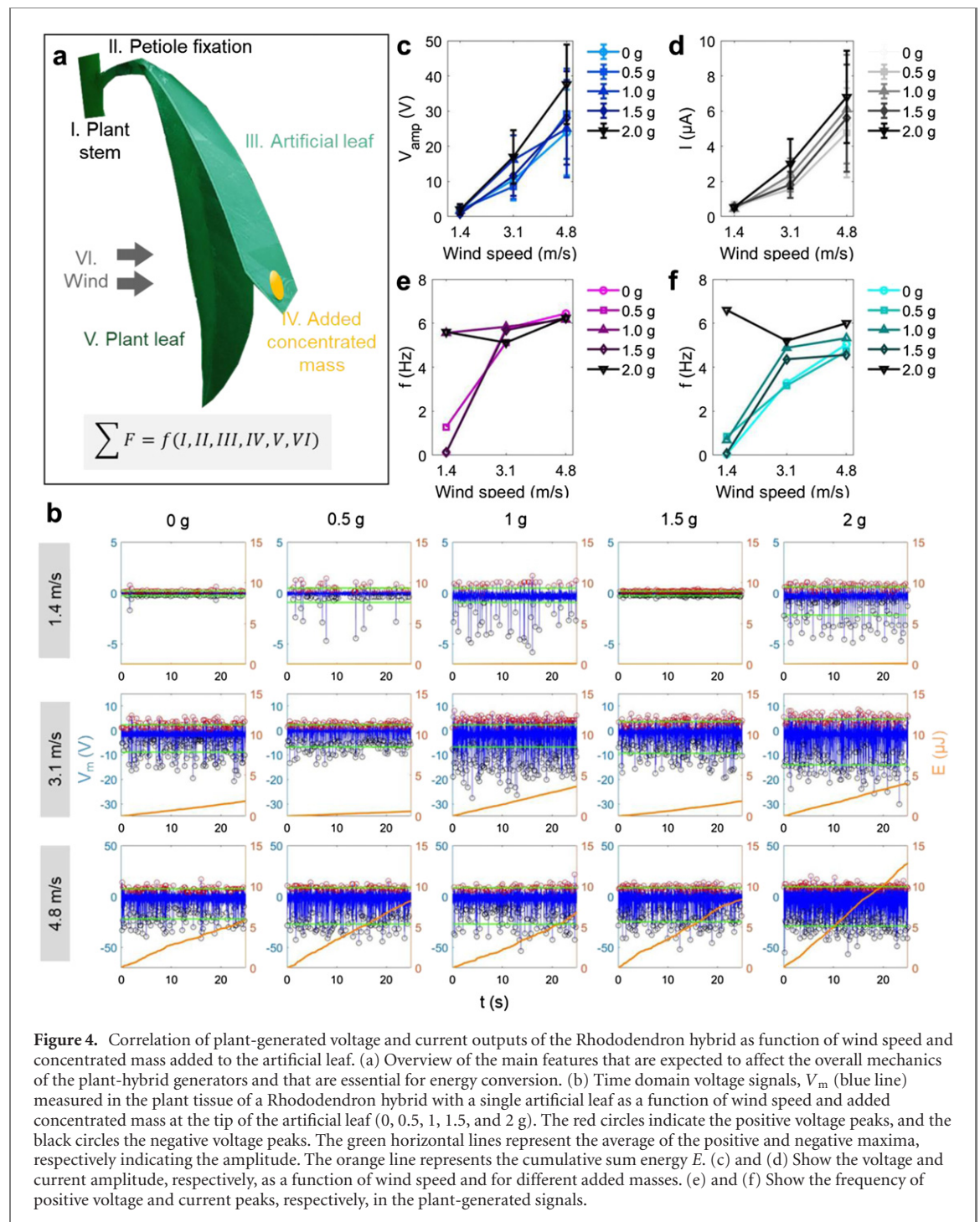
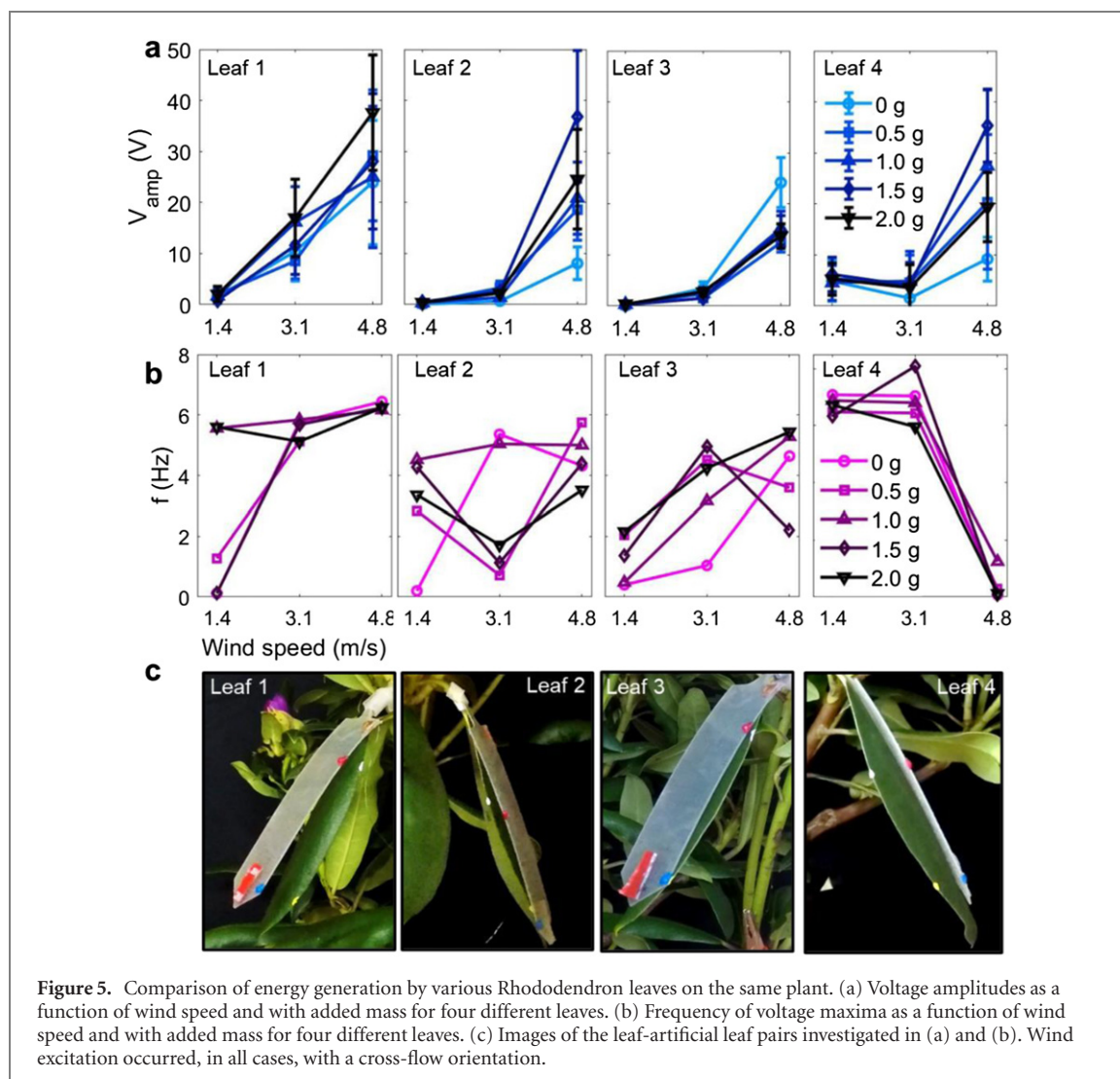


Figure 4. Correlation of plant-generated voltage and current outputs of the Rhododendron hybrid as function of wind speed and concentrated mass added to the artificial leaf. (a) Overview of the main features that are expected to affect the overall mechanics of the plant-hybrid generators and that are essential for energy conversion. (b) Time domain voltage signals, V_m (blue line) measured in the plant tissue of a Rhododendron hybrid with a single artificial leaf as a function of wind speed and added concentrated mass at the tip of the artificial leaf (0, 0.5, 1, 1.5, and 2 g). The red circles indicate the positive voltage peaks, and the black circles the negative voltage peaks. The green horizontal lines represent the average of the positive and negative maxima, respectively indicating the amplitude. The orange line represents the cumulative sum energy E . (c) and (d) Show the voltage and current amplitude, respectively, as a function of wind speed and for different added masses. (e) and (f) Show the frequency of positive voltage and current peaks, respectively, in the plant-generated signals.

speed. Sufficient separation between the artificial leaf and the natural leaf after contact is essential, as it is required for efficient charge separation and electrostatic induction. Indeed, when the leaves vibrate but do not separate sufficiently, i.e. they rest on top of each other during vibrations, voltage amplitudes are low. This confirms the idea that the individual leaf structure and its orientation with regard to the wind has a strong influence and is a key factor in the dynamics of energy production, together with wind speed. Undoubtedly, the shape and the materials of the artificial leaf determine its wind induced oscillations, and in our configuration, the cantilever piece of 5 mm

width located immediately after the petiole fixation likely has a major influence on the overall dynamics of the leaf. Similar to the petiole of a plant leaf, it allows not only vertical oscillations, but also torsional motions, as seen in the videos. In particular, high frequency but low voltage signals might be attributable to such torsional oscillations, as the separation is lower, and further investigations are required to determine the contributions of such torsional vibrations. Overall, the results confirm the essential influence of the parameters projected in figure 4(a), and among these, wind speed, natural leaf shape, artificial leaf shape, mass, and resulting vibrational properties are



essential factors influencing the electricity generated by the sequential contact and separation motions.

2.3. Outdoor wind-energy harvesting by plant-hybrid generators under natural conditions

The previous data confirm that our system is capable of converting air flow into electricity. Figure 6(a) shows an image of the outdoor application of the plant-hybrid generator consisting of a *Rhododendron* plant modified with eight artificial leaves that autonomously harvest real wind energy. Figure 6(b) gives an overview of the wind speed that was continuously measured during the experiment at the plant level (see position of anemometer in figure 6(a)). We measured an average wind speed of 1.9 m s^{-1} during the experiment ($\text{RH} \sim 69.3\%$ and $T = 13.9 \text{ }^\circ\text{C}$) and also periods of no/very low wind and gusts of up to a maximum of 5 m s^{-1} . The median wind speed hence corresponds to the lower wind speed in previous indoor experiments, which showed generally lower voltage signals. Figure 6(c) shows the

charging curves of eight $1 \text{ } \mu\text{F}$ capacitors connected to the plant and to the eight individual artificial leaves that were randomly assembled on leaves of a *Rhododendron* plant. The results indicate that the natural wind-driven leaf fluttering charges the capacitors with, as expected different charging dynamics being recorded for different leaves. The harvesting circuit discharges the capacitors automatically after reaching 2 V , corresponding to an energy stored in the capacitor of $2 \text{ } \mu\text{J}$ given by $E_{\text{cap}} = \frac{1}{2}CV^2$ where C is the capacitance and V the voltage of the capacitor. The fastest charging occurred with leaf 1, which reached 2 V within $t = \sim 14 \text{ s}$, corresponding to a power P of 143 nW when considering the capacitor being charged by a single leaf and when $P = E_{\text{cap}}/t$. The same artificial-leaf–natural-leaf assembly was also capable of powering 150 LEDs in wind with six artificial leaves in a configuration in which two leaves directly powered a panel with 50 LEDs each (video S5). Furthermore, the *Rhododendron* with eight artificial leaves powered a digital temperature sensor and display (see video S6).

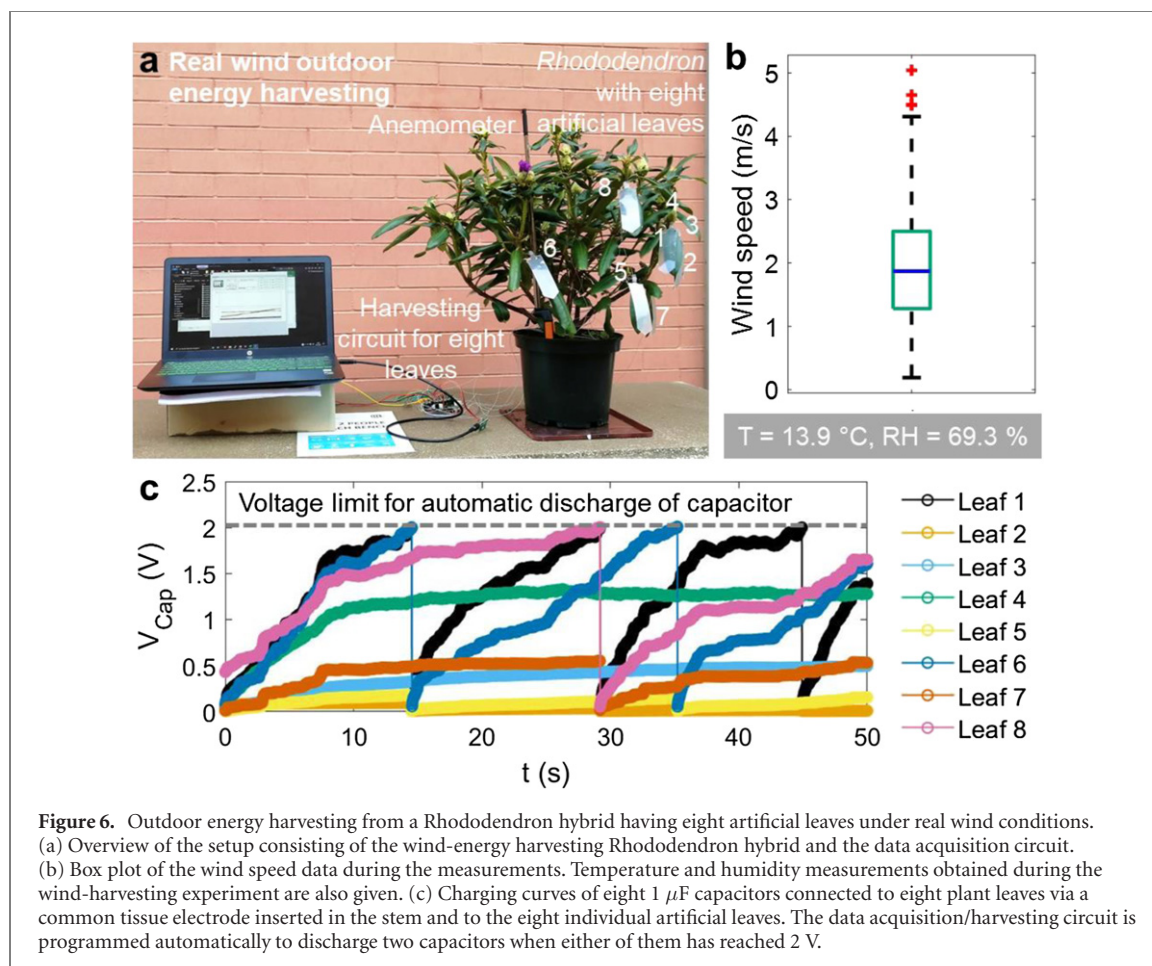


Figure 6. Outdoor energy harvesting from a *Rhododendron* hybrid having eight artificial leaves under real wind conditions. (a) Overview of the setup consisting of the wind-energy harvesting *Rhododendron* hybrid and the data acquisition circuit. (b) Box plot of the wind speed data during the measurements. Temperature and humidity measurements obtained during the wind-harvesting experiment are also given. (c) Charging curves of eight $1\ \mu\text{F}$ capacitors connected to eight plant leaves via a common tissue electrode inserted in the stem and to the eight individual artificial leaves. The data acquisition/harvesting circuit is programmed automatically to discharge two capacitors when either of them has reached 2 V.

3. Discussion

3.1. Leaf mechanics and tuning

The mechanical behavior of the *Rhododendron* leaf in combination with the artificial leaf within an air flow is highly complex because of the influence of multiple parameters related to the plant, the artificial leaf, and the wind excitation. Our results show that one of the key parameters impacting the generated signals is increasing wind speed (in cross-flow orientation), which typically increases the voltage and current signals and, in most cases, the frequency. A concentrated mass at the tip of the artificial leaf can sometimes have benefits, in particular, for achieving higher frequencies of the electrical signals generated even at low wind speeds. In addition, an optimum mass exists (in our case: 1 g) for obtaining a good balance of frequency and voltage amplitudes at all wind speeds. Changing the position of the concentrated mass on the artificial leaf is also expected to have an influence on the outcome. A concentrated mass has been shown to increase or decrease the critical flutter force of a beam depending on its location on the beam [30]. We have also observed that not only vertical but also torsional oscillations can occur that are caused by the combination of the blade and thin petiole in the natural leaf and the current design of the artificial leaf. The natural leaf and the artificial

leaf can perform torsional movements leading to flutter that can be used, in particular, for high frequency transient impacts [31, 32]. However, further tuning is required to improve the mechanical response based on individual plant leaves, as their geometry, which varies from leaf to leaf, influences the output strongly. Such tuning can be achieved by treating the geometrical and material parameters of the artificial leaf as design variables. In addition, consideration should be given to the design of artificial leaves that, in the same configuration, can adapt to the multiple morphologies of the natural leaves in order to avoid having to change the design for each and every leaf. Such adaptability might be achieved by soft structures capable of conformal contact with the leaf surface while retaining a certain elasticity ('springiness') to allow a suitably fast separation from the plant leaf. Moreover, our results have showed that sufficient separation after contact is essential for effective charge separation and induction in the tissue. Thus, after conformal contact, the structure should quickly separate from the plant leaf. Certainly, the natural leaf should not be damaged by these impacts. Further suggesting the application of soft materials (no leaf damage was observed under our conditions). Not only the behavior of the set-up may be optimized, but also its material chemistry as the latter can affect the output signals, and processes such as ion implantation (see figure

S2) and other surface modification can elevate the power output.

3.2. Outdoor energy harvesting

Our results show that real-wind outdoor energy harvesting is possible with the described system in which artificial leaves and the plant convert wind energy into electricity that can be accumulated in common capacitors. Further optimization of the mechanics and materials should elevate the overall outdoor applicability and power outputs of this system. However, further factors may play a role in an outdoor environment. For example, previous data have shown that humidity also influences signal generation by contact electrification, and lower humidity increases whereas higher humidity decreases the voltage amplitudes generated [3]. During our experiments, a relatively high RH of 70% was present including light rain up to 1 h before the experiment started. We consider that, under dryer conditions, higher outputs can be expected. The same previous study has also shown an influence of the wind direction on the output and suggests that a cross-flow orientation of leaf and wind direction leads to efficient oscillations and the highest power outputs [3]. In outdoor locations where changing wind directions are likely, the positioning of multiple leaves in various orientations on the plant can partially compensate for this effect, as we have confirmed by showing that not all leaves equally generate electricity. During the application of an artificial system under highly unstructured environmental conditions, such as on living plants, a certain variability is unavoidable, e.g. plant leaves will slightly differ in their size, morphology, and arrangement. Nevertheless, our results (and also those in reference [3]) demonstrate that a reproducible enhancement of the electricity, via the wind speed, is obtained in plants with combinations of natural and artificial leaves. The data also show that, in cross-flow orientation, some plant leaves charge faster than others, mainly because of their individual mechanical behavior. Notwithstanding, n equal artificial leaves all on the same plant should produce an expected (and desired) energy output for a given wind speed. Further tuning the self-adaptation of the interplay of artificial leaf with individual plant leaves might also improve the mechanical interactions and energy output. Hence, the optimization of the mechanics and the adaptation of the artificial leaf are essential targets for enhancing such outdoor signal generation. Even in its current state, the plant-generated electricity is sufficient instantaneously to power electric consumers such as LEDs and a temperature sensor in an air-flow. Further development of these autonomous power sources for reliable outdoor application on other plants and their combination with suitable electronics might lead to various sustainable sensing technologies, e.g. for agriculture, ecosystem monitoring, and in general, for linking plants to man-made electronic

technologies. The results also suggest that observation of leaf oscillations as a function of the wind speed in a location of interest before the installation of the entire system might predict its power output and suitability for that specific location.

4. Conclusions

Biohybrid generators in which common living plants constitute the main component for actively converting mechanical energy into electricity represent a possible small-scale ‘green’ autonomous power source. We have investigated the mechanical interplay of an artificial and a natural leaf and determined those parameters that play essential roles for achieving the highest voltage and current outputs in order to provide insights for the future design of such generators. Next to wind speeds, the morphology of the plant leaf and the design of the artificial leaf determine flutter-induced motions and interactions that influence higher energy outputs. We have shown, for the first time, that a *Rhododendron* plant with eight artificial leaves can autonomously accumulate electricity from real wind at low wind speed in an outdoor scenario and directly power 150 LEDs and a digital thermometer sensing circuit and display. The results reveal that living plant-based wind generators are potential autonomous power sources, for example, for low-power sensor networks and environmental monitoring.

Acknowledgments

This work was funded by the project GrowBot, the European Union’s Horizon 2020 Research and Innovation Programme under Grant Agreement No. 824074. TS acknowledges additional funding by the German Research Foundation (Deutsche Forschungsgemeinschaft, DFG) under Germany’s Excellence Strategy EXC-2193/1-390951807.

Data availability statement

The data that support the findings of this study are available upon reasonable request from the authors.

ORCID iDs

Fabian Meder  <https://orcid.org/0000-0002-1331-0265>

Marc Thielen  <https://orcid.org/0000-0002-7773-6724>

References

- [1] Lew T T S, Koman V B, Gordiichuk P, Park M and Strano M S 2020 *Adv. Mater. Technol.* **5** 1

- [2] Meder F, Must I, Sadeghi A, Mondini A, Filippeschi C, Beccai L, Mattoli V, Pingue P and Mazzolai B 2018 *Adv. Funct. Mater.* **28** 1806689
- [3] Meder F, Thielen M, Mondini A, Speck T and Mazzolai B 2020 *Energy Technol.* **8** 2000236
- [4] Kim D W, Kim S W and Jeong U 2018 *Adv. Mater.* **30** 1804949
- [5] Jie Y, Jia X, Zou J, Chen Y, Wang N, Wang Z L and Cao X 2018 *Adv. Energy Mater.* **8** 1703133
- [6] Wu H, Chen Z, Xu G, Xu J, Wang Z and Zi Y 2020 *ACS Appl. Mater. Interfaces* **12** 56060
- [7] Giraldo J P, Wu H, Newkirk G M and Kruss S 2019 *Nat. Nanotechnol.* **14** 541
- [8] Wong M H, Giraldo J P, Kwak S-Y, Koman V B, Sinclair R, Lew T T S, Bisker G, Liu P and Strano M S 2017 *Nat. Mater.* **16** 264
- [9] Kwak S-Y et al 2017 *Nano Lett.* **17** 7951
- [10] Di Giacomo R, Daraio C and Maresca B 2015 *Proc. Natl Acad. Sci. USA* **112** 4541
- [11] Kim J J, Allison L K and Andrew T L 2019 *Sci. Adv.* **5** eaaw0463
- [12] Stavrinidou E, Gabrielsson R, Gomez E, Crispin X, Nilsson O, Simon D T and Berggren M 2015 *Sci. Adv.* **1** e1501136
- [13] Stavrinidou E et al 2017 *Proc. Natl Acad. Sci. USA* **114** 2807
- [14] Thomas T, Lew S, Koman V B, Gordiichuk P, Park M and Strano M S 2019 *Adv. Mater. Technol.* **5** 1900657
- [15] Nitisoravut R and Regmi R 2017 *Renew. Sustain. Energy Rev.* **76** 81
- [16] Strik D P B T B, Timmers R A, Helder M, Steinbusch K J J, Hamelers H V M and Buisman C J N 2011 *Trends Biotechnol.* **29** 41
- [17] Strik D P B T B, Hamelers H V M, Snel J F H and Buisman C J N 2008 *Int. J. Energy Res.* **32** 870
- [18] Deng H, Chen Z and Zhao F 2012 *ChemSusChem* **5** 1006
- [19] McCormick A J, Bombelli P, Bradley R W, Thorne R, Wenzel T and Howe C J 2015 *Energy Environ. Sci.* **8** 1092
- [20] Mershin A, Matsumoto K, Kaiser L, Yu D, Vaughn M, Nazeeruddin M K, Bruce B D, Graetzel M and Zhang S 2012 *Sci. Rep.* **2** 234
- [21] Tschörtner J, Lai B and Krömer J O 2019 *Front. Microbiol.* **10** 866
- [22] Flexer V and Mano N 2010 *Anal. Chem.* **82** 1444
- [23] Miyake T, Haneda K, Nagai N, Yatagawa Y, Onami H, Yoshino S, Abe T and Nishizawa M 2011 *Energy Environ. Sci.* **4** 5008
- [24] Riederer M and Müller C 2006 *Biology of the Plant Cuticle* ed M Riederer and C Müller (Oxford: Blackwell)
- [25] Yeats T H and Rose J K C 2013 *Plant Physiol.* **163** 5
- [26] Lowell J and Rose-Innes A C 1980 *Adv. Phys.* **29** 947
- [27] Wu C, Wang A C, Ding W, Guo H and Wang Z L 2019 *Adv. Energy Mater.* **9** 1802906
- [28] Wang Z L 2013 *ACS Nano* **7** 9533
- [29] Wang Z L, Chen J and Lin L 2015 *Energy Environ. Sci.* **8** 2250
- [30] Sohrabian M, Ahmadian H and Fathi R 2016 *Lat. Am. J. Solids Struct.* **13** 3005
- [31] Tadrist L, Julio K, Saudreau M and De Langre E 2015 *J. Fluids Struct.* **56** 1
- [32] Amandolese X, Saudreau M, He P, Leclercq T and De Langre E 2018 *J. R. Soc. Interface* **15** 20180010